

cluded from Figs. 2 and 3 and the analytic representations. The 19 mm tubes were furthermore found to have a different type of calibration curve, and they have also been excluded from the analytic representations. The five 19 mm tubes showed no variation in the tested range of relative lengths, and this observation was confirmed by the extra 10 mm tube used. This is not a final proof that there is no dependence at smaller tube diameters, but it is a clear indication.

The results can be represented by the least-squares fit

$$\frac{\Delta p}{\tau} = 87.77 \cdot \log_{10} \left[ \frac{u \tau^D}{\nu} \right] - 51.93 \quad 50 < \frac{u \tau^D}{\nu} < 1000$$

or

$$\frac{\Delta p}{\tau} = 38.85 \cdot \log_{10} \frac{\Delta p D^2}{\rho \nu^2} - 111.92$$

$$2.5 \cdot 10^5 < \frac{\Delta p D^2}{\rho \nu^2} < 2.1 \cdot 10^8$$

It should be observed that reducing the data directly from experimental points expressed as  $\Delta p/\tau$  vs  $d^*$ , gives a different result from curve-fitting  $x^*$ ,  $y^*$  values and then transforming to  $\Delta p/\tau$ ,  $d^*$ .

Figure 3 shows the scatter in estimated  $C_f$  resulting from the scatter in the calibration experiments. The standard deviation in 0.022. For the point illustrated in Fig. 1 with an "uncertainty rectangle", the values obtained are  $C_{f_{exp}}/C_{f_{cal}} = 0.89 - 1.04$ .

The pressure magnitudes were: dynamic pressure based on maximum velocity:  $U_e$  101 N/m<sup>2</sup>; Dynamic pressure based on mean velocity  $\bar{U}$  69 N/m<sup>2</sup>; Preston tube indicated pressure  $\Delta p_e$  34 N/m<sup>2</sup>; and static pressure range 2 N/m<sup>2</sup>.

### Conclusions

The results of the present investigation show that: in terms of  $x^*$ ,  $y^*$  variables the results of Patel are, not unexpectedly, verified. The differences between existing calibration curves fall within an "uncertainty rectangle" for plausible choices on how static pressure and pressure drop measurements can be performed.

Greater accuracy can be obtained with new variables. A calibration based on present data gives straight line fit in wall variables  $\Delta p/u_\tau$  and  $u_\tau D/\nu$ . The relative length is unimportant in the region tested, down to  $L/D = 1.6$ .

### References

- Rechenberg, I., "Messung der turbulenten Wand-schubspannung," *Zeitschrift für Flugwiss.*, Vol. 11, Heft 11, Nov. 1963, pp. 429-438.
- Preston, J.H., "The Determination of Turbulent Skin Friction by Means of Pitot Tubes," *Journal Royal Aeronautical Society*, Vol. 58, Feb. 1954, pp. 109-121.
- Patel, V.C., "Calibration of the Preston Tube and Limitations on its Use in Pressure Gradients," *Journal of Fluid Mechanics*, Vol. 23, Part 1, Sept. 1965, pp. 185-208.
- Hopkins, E.J. and Keener, E.R., "Study of Surface Pitots for Measuring Turbulent Skin Friction at Supersonic Mach Numbers-Adiabatic Wall," NASA TN D-3478, July 1966.
- Allen, J.M., "Evaluation of Preston Tube Calibration Equations in Supersonic Flow," NASA TN D-7190, May 1973. Synopsis in *AIAA Journal*, Vol 11, Nov. 1973, pp. 1461-1462.
- Head, M.R. and Vasanta Ram, V., "Simplified Presentation of Preston Tube Calibration," *Aeronautical Quarterly*, Vol. 22, Part 3, Aug. 1971, pp. 295-300.
- Bradshaw, P. and Unsworth, K., "A Note on Preston Tube Calibrations in Compressible Flow," Imperial College Aero Rept. 73-07, London, 1973.
- Bertelrud, A., "Pipe Flow Calibration of Preston Tubes of Different Diameters and Relative Lengths Including Recommendations on Data Presentation for Best Accuracy," Aeronautical Research Institute of Sweden, Bromma, Sweden, FFA Rept. 125, 1974.

<sup>9</sup>Ozarapoglu, V., "Measurements in Incompressible Turbulent Flows," Doctoral Thesis, University of Laval, Quebec, Canada, Feb. 1973.

<sup>10</sup>Schlichting, H., *Boundary-Layer Theory*, 6th ed., McGraw-Hill, New York, 1968, p. 574.

<sup>11</sup>Private communication.

<sup>12</sup>Smith, D. and Walker, J., "Skin-Friction Measurements in Incompressible Flow," NASA TR R-26, 1959.

## Experimental Investigation of Boron/Lithium Combustion

R. Mestwerdt\* and H. Selzer†

DFVLR Institut für chemische Raketenantriebe  
Standort Trauen, West-Germany

### Introduction

**A**IR augmented rockets offer some advantages for long propelled missions in comparison to conventional rockets. The necessary reduction of the tank-weight and the high heat of combustion favor the use of boron as a fuel. Unfortunately, the complete reaction of boron in air can only be achieved if the ignition temperature is higher than 1950 K, otherwise a dense shielding oxide layer will be formed preventing further fast oxidation.

To overcome these difficulties, several approaches are being studied: a) to control the total reaction process in a way that the boron particles are heated up to 1950 K in a fuel rich environment; b) to modify the reaction process by the formation of different intermediates as for example in the presence of OH-radicals; and c) to treat the boron itself in order to avoid a closed oxide layer.

As the first two approaches are being studied by Schadow<sup>1,2</sup> and Boussios,<sup>3</sup> the third area of investigation will be reported here. From theoretical considerations the system boron/lithium looked very promising.<sup>4,7</sup> Attempts to coat the boron had been not successful in avoiding combustion problems, therefore a binary metal compound was used. Neither the Li/B product could be ordered nor a description found on how to produce it. Thus, the first step was to find a way to produce a co-melt of Li/b.

### Experiments

Figure 1 illustrates the small oven used to produce the compound. About 1.5 g of crystalline boron (purity 98/99%) was placed in a tantalum cylinder together with lithium particles in argon atmosphere. The cell was sealed and heated up to 900 K in vacuum in order to avoid oxidation of the tantalum and to measure the heat of formation of the Li-B compound by the analysis of the temperature/power plot. The molar ratios (Li:B) investigated were between 1:2 and 1:6. After the reaction, the cell contained two different materials: a granular part which was mainly boron, and a hard compact body which consisted of one part lithium and two parts boron. The product LiB<sub>2</sub> is oxidized in air and had to be stored therefore in argon.

To run the tests at temperatures higher than 2000 K an electrical resistance-furnace was selected using a graphite tube. A

Presented as Paper 75-247 at the AIAA 13th Aerospace Sciences Meeting, Pasadena, Calif., January 20-22, 1975; submitted March 7, 1975; revision received May 5, 1975.

Index categories: Fuels and Propellants, Properties of; Combustion in Heterogeneous Media.

\*Phys.-Ing. (grad), Deutsche Forschungs-und Versuchsanstalt für Luft- und Raumfahrt e.V.

†Doctor rerum, naturalium, ERNO Raumfahrt GmbH.

Table 1 Physical properties of some metal and their oxides.

Metal	Melting Point of the		Boiling Point of the		Density	Heat of Combustion			
	Metal in K	Oxide in K	Metal in K	Oxide in K		kJ/g Metal	kJ/cm <sup>3</sup> Metal		
Li	454	(Li <sub>2</sub> O)	1700	1620	(Li <sub>2</sub> O)	3200	0,53	43,29	22,94
Mg	923	(MgO)	3075	1381	(MgO)	3350	1,74	24,78	43,12
Al	932	(Al <sub>2</sub> O <sub>3</sub> )	2318	2740	(Al <sub>2</sub> O <sub>3</sub> )	3800	2,70	31,08	83,92
Be	1556	(BeO)	2823	2750	(BeO)	4123	1,84	66,36	122,10
B	2300	(B <sub>2</sub> O <sub>3</sub> )	723	3950	(B <sub>2</sub> O <sub>3</sub> )	2520	2,35	58,48	137,43
LiB <sub>2,5</sub>	?	-	?	-	-	-	1,84	55,09	101,37

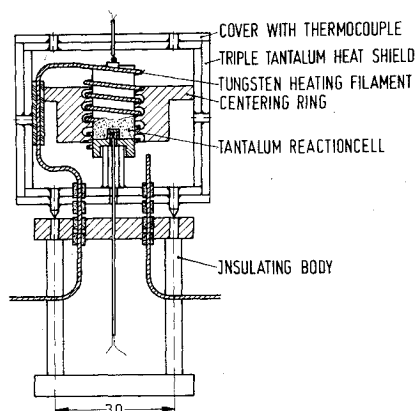


Fig. 1 High temperature furnace for producing boron/lithium fuel.

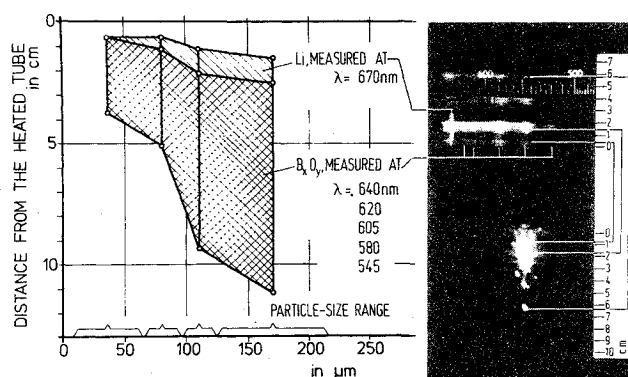


Fig. 3 Spectral intensity and lifetime of boron/lithium particles.

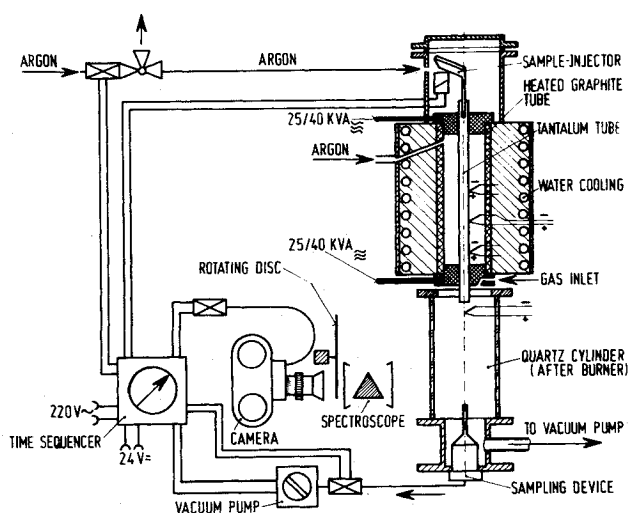
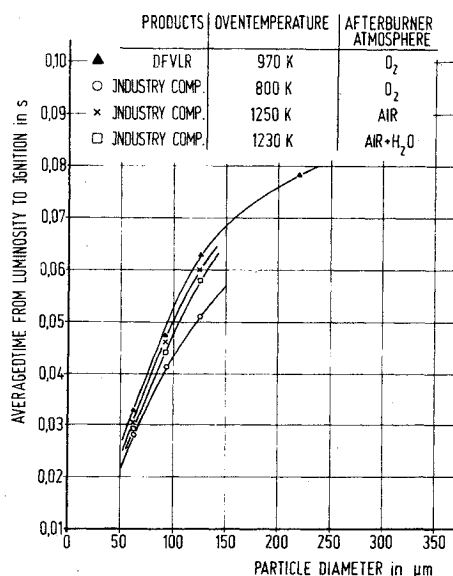


Fig. 2 Scheme of the experimental set up for ignition and combustion tests.

Fig. 4 Ignition delaytime of boron/lithium particles (Particle-velocity  $V = 6.2$  m/s).

thin tantalum-tube was placed in the centerline to exclude the influence of the partial pressure of carbon on the boron. A steady argon-flow prevented the oxidation of the tantalum.

As Fig. 2 illustrates, the particles to be tested were shot through the tantalum tube into a quartz-cylinder serving as an after burner filled with the test gases. About 4 mg metal particles were used per test. The injection velocity was 6.2 m/sec. The ignition and combustion of the particles were analyzed by photographic equipment and spectrography. The combustion products were collected at the bottom or scraped from the wall of the cylinder and chemically analyzed or studied in a scanning electron microscope.

### Results

Care was taken to determine the temperature profile of the particles in the centered tube and the influence of the cold outlet. It was estimated that the particles were roughly on the

order of 100°C cooler than the oven-temperature. The data presented in the figures are oven-temperatures.

It was also very difficult to determine an accurate ignition temperature since in most cases it will be a function of the reaction rate desired. The tests showed that the ignition temperature is dependent on the chemical quality of the particles and on the mixture ratio of the homogeneous after burner gases (ratio of air to oxygen mass flow). Although this judgment is highly subjective, the variation of the oven-temperature enabled a rather easy decision of the lowest value for a complete reaction.

Figure 3 represents the application of the combustion diagnostic by spectral analysis. The general flame behavior was as follows: after the induction period, the reaction started with lithium followed by the intense boron-flame. The spectral analysis supported the color-interpretation of the traces. The ignition delay depended on the particle size range, yet the

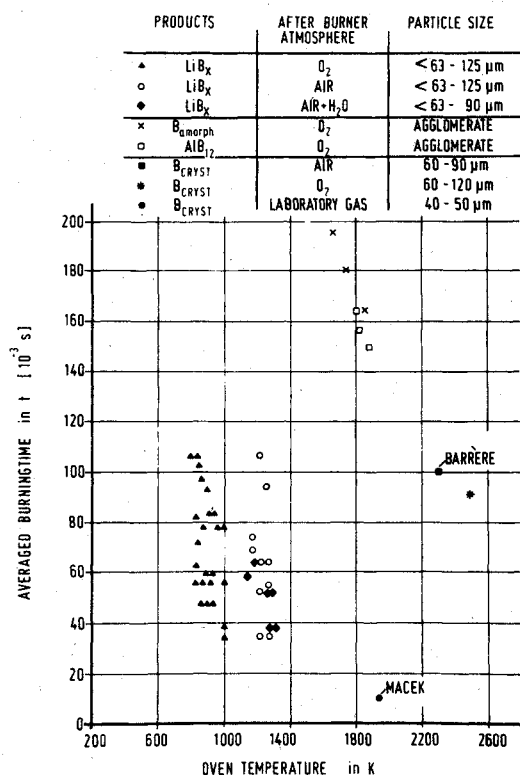


Fig. 5 The burning time of particles as a function of the oven temperature.

lithium could also be observed in the later phase of the particle burning-time. Thus a steady consumption of both the lithium and boron can be assumed for the main combustion. The findings of the spectral analysis were supported by the chemical analysis of the condensate from the quartz wall. Close to the exit of the oven, mainly lithium was identified. Further downstream in the combustion both lithium and boron could be detected.

The ignition delay time was plotted in Fig. 4. It varied from 30 msec Fig. 4 to 80 msec depending on the best conditions. The averaged burning time increased with increasing particle diameter. A comparison with the findings of other authors for pure boron was made in Fig. 5. The heat of combustion was measured in a calorimetric bomb to be 52.46 KJ/g.

### Discussion

The ignition temperature of boron could be lowered from 2500 K to 800 K by using a  $\text{LiB}_{2.5}$  compound. This ignition temperature was slightly increased by using air or humid air (90% moisture) instead of pure oxygen. The difficulties encountered for a complete combustion can best be discussed by using Table 1. The boiling temperature of the metal boron (3950 K) is much higher than that of the oxide  $\text{B}_2\text{O}_3$  (2520 K) forming a dense layer above the melting point at 723 K. Therefore, a fast oxidation can only take place if the shielding oxide layer has been destroyed. The combined use of boron and lithium resulted in a very low ignition temperature (about 900°C in air) and complete combustion. The reaction mechanism was interpreted by the start-up phase of a lithium flame heating up the particle to the onset of the boron reaction. A closed oxide layer could not form as the lithium continued to vaporize or as lithiumborate was formed. All photographs showed a smooth combustion around the particles and no spinning traces as in the case of aluminum. These findings of good ignition and combustion properties together with a high heat of combustion justify further investigations of the B/Li compound as a prominent candidate for use within air-augmented propulsion systems.

### References

- <sup>1</sup>Schadow, K., "Study of Gaseous Nonequilibrium Effects in Particle-Laden, Ducted Flows for Improvement of the Combustion Efficiency," AIAA Paper 72-36 San Diego, Calif., 1972.
- <sup>2</sup>Schadow, K., "The Influence of Combustor Parameters on the Combustion of Particle-Laden Fuels in Ducted Flows," AIAA Paper 73-177, Washington, D.C., 1973.
- <sup>3</sup>Boussios, A., "Primärkammerprozesse für Kombinationsantriebe," Kursus der Carl-Cranz-Gesellschaft über "Flugkörperantriebe" in Braunschweig, March 19-23, 1972.
- <sup>4</sup>McLain, W.H., "Identification of Exhaust Species from the combustion of LM and LMH Fuels," AFRPL TR-68-105, April 1968, Air Force Rocket Propulsion Lab., Edwards Air Force Base, Calif.
- <sup>5</sup>Markowskii, L.Ya. and Kondrashev, Yu.D., "The composition and Properties of Borides of the Elements of the first and second Groups of the periodic Systems," *Zhurnal Neorganicheskoi Khimii*, Vol. 11, No. 1, 1957, pp. 34-41.
- <sup>6</sup>Secrist, Childs, US Atomic Energy Rept. TID-17149, 1962.
- <sup>7</sup>Hsia, H., "Air-Augmented Combustion of Boron and Boron-Metal Alloys," Final Rept. AFR DL-TR-71-80, June 1971, Air Force Research Lab., Wright-Patterson Air Force Base, Ohio.

## Detection of Boundary-Layer Transition with a Laser Beam

A. J. Laderman\* and A. Demetriades†  
Aeronutronic Ford Corporation,  
Newport Beach, Calif.

### Introduction

SEVERAL techniques, including surface sensors,<sup>1</sup> external probes<sup>2,3</sup> and optical methods<sup>3,4</sup> have been used for detection of transition in high speed, compressible boundary layers. While the various techniques yield useful information, each is deficient in some respect. Surface sensors, for example, respond only to phenomena adjacent to the wall, while probes (e.g. hot-wires) must be considerably smaller than the boundary-layer thickness  $\delta$  in order not to disturb the local flow. Optical methods (schlieren, shadowgraph) are generally only qualitative in nature.

This Note describes an alternative scheme which overcomes these limitations. It involves the use of a laser beam in place of conventional optics, whose distortion by turbulence can be quantitatively linked to transition. Since the beam does not disturb the flow and can be focused to a region much smaller than  $\delta$  it has potential for probing the entire transition region with high resolution. The feasibility of the method has been demonstrated using a helium-neon laser, with a beam approximately 1 mm diam, directed through a Mach 3 boundary layer. The beam axis is aligned parallel to the floor of the wind tunnel over which the boundary layer is growing and normal to the direction of mean flow, and is imaged on the plane of an apertured detector. In the direction of light propagation, therefore, the mean flow is uniform while both the mean flow and optical gradients are large in the direction normal to the wall and to the light beam.

### Analysis

To assess the effects of turbulence on the optical quality of the beam, it can be assumed that the beam has a Gaussian

Received March 13, 1975; revision received July 14, 1975.

Index categories: Boundary Layers and Convective Heat Transfer—Turbulent; Boundary Layer Stability and Transition; Supersonic and Hypersonic Flow.

\*Principal Scientist, Experimental Fluid Mechanics Section. Member AIAA.

†Supervisor, Experimental Fluid Mechanics Section. Associate Fellow AIAA.